JOINT TIME-FREQUENCY-SPACE CLASSIFICATION OF EEG IN A BRAIN-COMPUTER INTERFACE APPLICATION

Gary Garcia Molina, Touradj Ebrahimi and Jean-Marc Vesin

Swiss Federal Institute of Technology - EPFL, CH-1015 Lausanne, Switzerland
Gary.garciamolina@epfl.ch, Touradj.Ebrahimi@epfl.ch,
Jean-Marc.Vesin@epfl.ch

Abstract: Brain-computer interface is a growing field of interest in Human Computer Interaction with divers applications ranging from medicine to entertainment.
In this paper, we present a system which allows for classification of mental tasks based on a joint time-frequency-space decorrelation, in which mental tasks are measured via electroencephalogram (EEG) signals. The efficiency of this approach was evaluated by means of real-time experimentations on two subjects performing three different mental tasks. To do so, a number of protocols for visualization, as well as training with and without feed-back were also developed. Results obtained show that it is possible to obtain good classification of simple mental tasks, in view of command and control, after a relatively small amount of training, with accuracies around 80%, and in real-time.
Keywords: Brain Computer Interface, EEG, Multivariate signals classification, Ambiguity function, Simultaneous diagonalization.

1. INTRODUCTION

Research on Human-Computer Interfaces (HCI) for disabled people has lead to the so called Brain-Computer Interface (BCI) systems that use brain activity for communication purposes. When the brain activity is monitored through electroencephalogram (EEG) measurements one has an EEG-based BCI, henceforth called simply BCI.

Current BCIs use the following non-invasive EEG signals:

- Event Related Potentials (ERP), which appear in response to some specific stimulus. ERPs can provide control when the BCI produces the appropriate stimuli. The advantage of an ERP based BCI is that little training is necessary for a new subject to gain control of the system. The disadvantage is that the subject must wait for the relevant stimulus presentation [1].
- Steady-State Visual-Evoked Responses (SSVER) which are elicited by a visual stimulus that is modulated at a fixed frequency. The SSVER is characterized by an increase in EEG activity at the stimulus frequency. With biofeedback training, subjects learn to voluntarily control their SSVER amplitude. Changes in the SSVER result in control actions occurring at fixed intervals of time [2].
- Slow Cortical Potential Shifts (SCPS) that are shifts of cortical voltage, lasting from a few hundred milliseconds up to several seconds. Subjects can learn to produce SCPS amplitude shifts in an electrically positive or negative direction for binary control. This skill can be acquired if the subjects are provided with a feedback on the course of their SCP and if they are positively reinforced for correct responses [3].
- Spontaneous signals (SS) that are recorded in the course of ordinary brain activity. These signals are spontaneous in the sense that they do not constitute the responses to a particular stimulus.

A BCI based on spontaneous signals generates a control signal at given intervals of time based on the classification of EEG patterns resulting from a particular mental activity [4] [5].

The development in BCI research was mainly motivated by the hope that it could serve as an augmentative communication option for people with motor disabilities [6]. However, efficient BCIs can serve as additional command and control means when the hands are used for other tasks, as in the case of pilots. The application that motivated our research was the design of an immersive environment where people could interact, between themselves and the environment, by simply thinking.

The achievement of a successful BCI system depends on system design factors (classification algorithm, communication bit-rate and feedback strategy) as well as on subject motivation.

There is a subject-dependency because the subject should learn how to control his EEG in order to interact with the system. Human factors such as fatigue, stress or boredom are of great influence; one of the first questions when designing a BCI should be how to motivate the subject.

In this paper we present a time-frequency SS-based BCI. We designed five operational modes (OM) going from the simple real-time visualization of EEG in a 3D environment to object-control. In this way the subject can become familiar with the system and get motivated because of the 3D environment where the interaction takes place.

2. GENERAL CONCEPTS

A BCI can be defined as a communication system that involves two entities: a human subject and a machine. The subject communicates by producing EEG and the machine responds with "actions". In this research the machine is a computer and the computer actions are dynamic multimedia signals (3D scenes, images, videos or sounds).

The subject performs mental activities to control the computer actions. These mental activities are characterized by the presence of patterns in recorded EEG signals.

The correspondence between EEG patterns and computer actions constitutes a machine-learning problem since the computer should learn how to recognize a given EEG pattern. In order to solve this problem a training phase is necessary, in which the subject is asked to perform mental activities and a computer algorithm is in charge of extracting the EEG patterns characterizing them.

When the training phase is finished, the subject can start to control the computer actions with her/his thoughts. This is the application phase and constitutes the ultimate goal of our research.

2.1 EEG acquisition

EEG signals are measured at the scalp by affixing an array of electrodes according to the 10-20 international system (Figure 1) and with reference to digitally linked ears (DLE).

DLE voltages are obtained by using the average of voltages at both ear-lobes as reference. The ear-lobes are selected because they constitute an almost quiet reference. In fact, they present small influences due to temporal activity [7].

If we note V_e the voltage at any of the electrodes, V_{A_1} and V_{A_2} the voltages at left ear lobe and right ear lobe respectively, then the DLE referenced voltage of electrode "e" is:

$$\begin{aligned} V_e^{DLE} &= \left(V_e - V_{A_1}\right) - \frac{1}{2}\left(V_{A_2} - V_{A_1}\right) = V_e - \frac{1}{2}\left(V_{A_1} + V_{A_2}\right) \quad \text{when } V_{A_1} \text{ is the physical reference} \\ &= \left(V_e - V_{A_2}\right) - \frac{1}{2}\left(V_{A_1} - V_{A_2}\right) = V_e - \frac{1}{2}\left(V_{A_1} + V_{A_2}\right) \quad \text{when } V_{A_2} \text{ is the physical reference} \end{aligned} \tag{1}$$

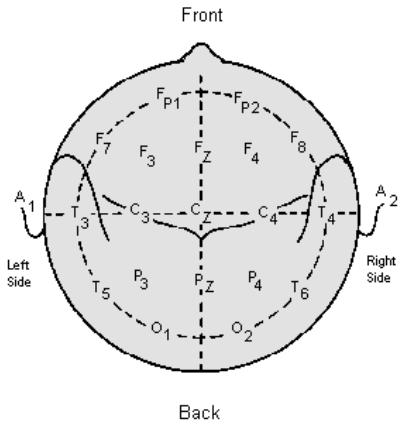

Figure 1. International 10-20 system of electrodes-placement.

An EEG signal is thus composed of the DLE-signals of each electrode. When a measure is composed of such single composite measures it is called multivariate [8].

2.2 Training phase

The objective of this phase is two-fold: to extract EEG patterns that uniquely characterize mental activities (MA), and to train the subject. The results of this phase are MA models that will serve as references for the application phase.

This phase can be performed with two approaches, namely training without feedback and training with feedback.

In the case of training without feedback, the subject is asked to perform MAs during a given amount of time (with repetitions if necessary) while his EEG signals are recorded for ulterior MA model construction.

In the case of training with feedback clue information is provided to the subject that tells him if his EEG pattern was successfully identified (positive feedback) or not (negative feedback). According to neuroscience results [9] [10] the human brain is able to modulate its activity in order to minimize the number of negative feedbacks. Training with feedback is possible only if an MA model exists, i.e. the information of a previous training without feedback is available.

2.3 Application phase

The basic scheme of a BCI in its application phase is shown in Fig. 2. The computer action at recognition time t_k is generated by the classification of the EEG pattern present in the EEG signals (S_k) recorded during the T seconds preceding the recognition time. In the sequel, we will call this EEG segment of duration T a trial.

The time interval, between two successive recognition times is noted T_I (interaction period or computer actions period). The choice of T_I and T is the result of a tradeoff between computer actions rate, EEG pattern misclassification probability and computational cost.

As EEG signals are contaminated by noise, a preprocessing step is necessary. The trial S_k is then passed trough the preprocessing module whose output is a clean trial X_k or a special message if S_k is too perturbed to be useful.

The pattern estimation module extracts the EEG patterns F_k contained in X_k. The nature of F_k is determined by the classification algorithm.

Finally a classifier module decides which computer action to consider based on a distance measure between MA model representatives and the pattern F_k.

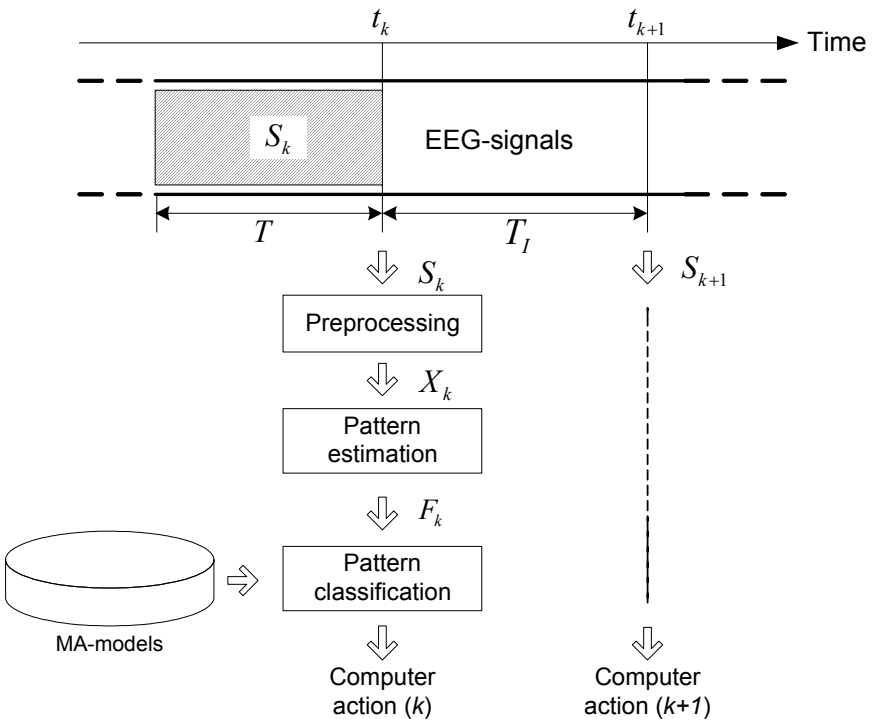

Figure 2. Basic scheme of a BCI in its application phase.

3. PROPOSED BCI-SYSTEM

3.1 BCI-system modules

According to Fig. 2, a BCI in its application phase is composed of the following modules: *signal-acquisition*, *preprocessing*, *pattern estimation*, *pattern classification* and *computer actions generator*.

In the training phase, the same modules are used plus an MA model builder. The role of the computer actions generator is however different here as it is used to display visual cues (indicating which MA to perform) and to provide feedback.

Since BCI technology is still in its experimental phase these modules and their relationships should be as flexible as possible.

3.2 Operational modes of the BCI

Five operational modes (OM[1]) were implemented; they allow the subjects to perform various experiments from simple to more complex.

Visualization OM (VOM): in this OM, the subject can watch a visual representation of his EEG in real time. Specific EEG features, such as the power values in the typical frequency bands (δ, θ. α. β), inter-electrode coherences, and total power at a given electrode are mapped to a 3D virtual environment, and regularly updated. The objectives of this OM are to familiarize the subject with the system as well as to calibrate the latter.

Training without feedback OM (NFOM): in this OM, the subject is asked (by means of visual or audio cues) to perform a defined mental activity. The produced EEG is then recorded for offline MA model construction.

Training with feedback OM (FOM): The subject is asked to perform an MA and a feedback is provided. This feedback is positive when the computer recognizes the mental activity and negative

[1] In a previous paper [11] the operational modes were called experiments.

otherwise. That is possible as MA models were calculated during a previous training without feedback. MA models can be updated in the course of a FOM (dynamic update) or at the end of it [11].

Control OM (COM): Since the results of previous OMs are MA models, the subject can start to control the system by performing the mental activities for which the system has been trained. In this OM, visual or sound cues are no longer necessary.

Multi-subject simultaneous training OM (MUOM): This is a particular form of the FOM. It consists in a multi-subject game whose goal is to gain the control of an object by performing an MA. This OM was chosen, because of its more stimulating effect when compared to a simple feedback.

3.3 System architecture

We grouped the system modules listed before into three components: signal-production, signal-processing and multimedia renderer.

We propose a distributed architecture in which each component offers specific services to the others in an efficient and transparent way.

Figure 3 depicts the architecture diagram of our BCI system.

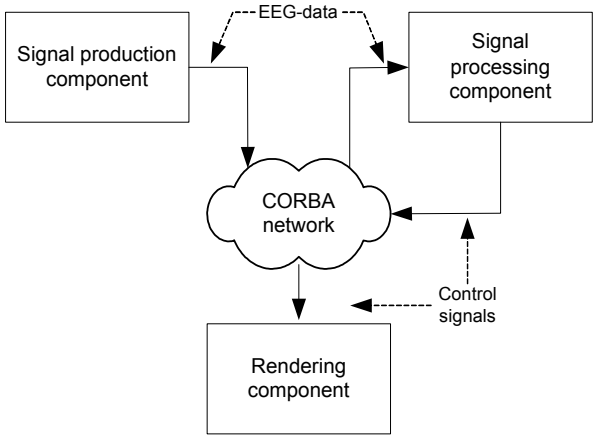

Figure 3. BCI-system architecture.

1- The s*ignal production component* is responsible for signal acquisition, digitalization and efficient data transmission through the network.

2- The signal processing component is in charge of signal preprocessing, pattern extraction, MA model construction and pattern classification.

3- The rendering component is used to display multimedia cues in NFOM and FOM, as well as to provide the feedback for the FOM. Furthermore, it acts as renderer in the VOM, COM and MUOM.

The communication rules between these components were designed over the CORBA [12] specification and implemented in JAVA (for networking) and C and MATLAB (for processing).

4. EEG SIGNALS PREPROCESSING

The purpose of EEG signal preprocessing is to maximize the signal-to-noise-ratio (SNR). Noise sources can be non-neural (eye movements, muscular activity, 50 Hz power-line noise) or neural (EEG features other than those used for control) [6].

In this research, we centered our analysis on non-neural noise such as eye-movement artefacts, muscular artefacts and the 50 Hz power-line noise.

Since the frequencies of interest in EEG are mainly located below 40 Hz, we filtered the signals between 1 and 40 Hz. The 50 Hz power-line noise was therefore attenuated.

For eye-movement artefacts and muscular artefacts we chose to reject a trial containing any of these artefacts and consequently such a trial could not generate any computer action.

In the case of muscular activity, one of the best approaches for detection consists in using Independent Component Analysis (ICA) of EEG. However, ICA is basically an offline method since it is only meaningful when the amount of data is large enough [13].

A practical method for detecting muscular artefacts is based on the fact that these artefacts are characterized by high frequencies (above 20 Hz) and high amplitudes. In [14] muscle artefact detection is achieved by considering the absolute and relative power over 25 Hz. In this work, we set a threshold on the power at this frequency band based on visual inspection and ICA during a calibration step.

For eye-movement artefacts detection many methods have been proposed [15]. They are fundamentally offline because they are mainly oriented to clinical research.

We implemented a method based on the power at prefrontal electrodes (Fp1 and Fp2) because eye-movement artefacts are characterized by an abrupt change in amplitude mainly localized at Fp1 and Fp2 (Fig. 4). The signal power at Fp1 and Fp2 is computed every half-second and compared to the mean power of the preceding two seconds. If the current power subtracted from the mean is larger than some multiple of the standard deviation of the two-second power, the trial is marked as contaminated by an eye artefact and thus rejected. The threshold is determined in the calibration step.

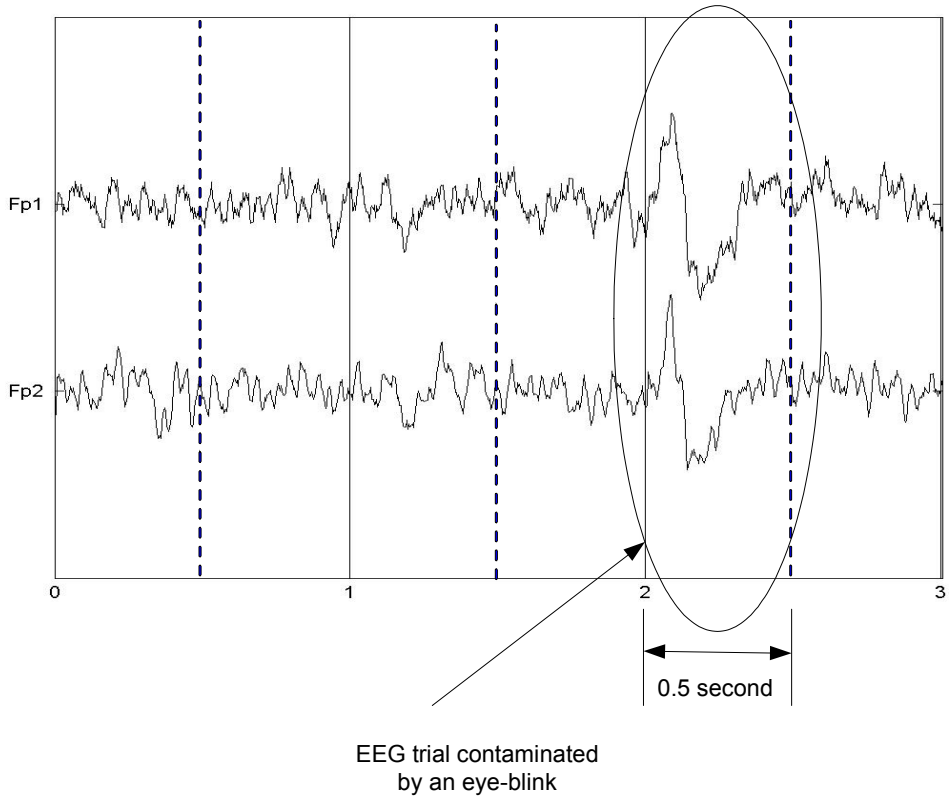

Figure 4. Rejection of an EEG trial contaminated by an eye-blink artefact.

5. EEG SIGNALS CLASSIFICATION

The classification of EEG signals based on the patterns characterizing the MAs constitutes a fundamental part of a BCI. As a matter of fact, the choice of the temporal parameters T and T_1 is strongly dependent on the classification method.

An EEG signal is multivariate because it is composed of signals coming from several electrodes. In this paper, we propose a decomposition of the multivariate classification into univariate classifications. Figure 5 depicts the general scheme of our method.

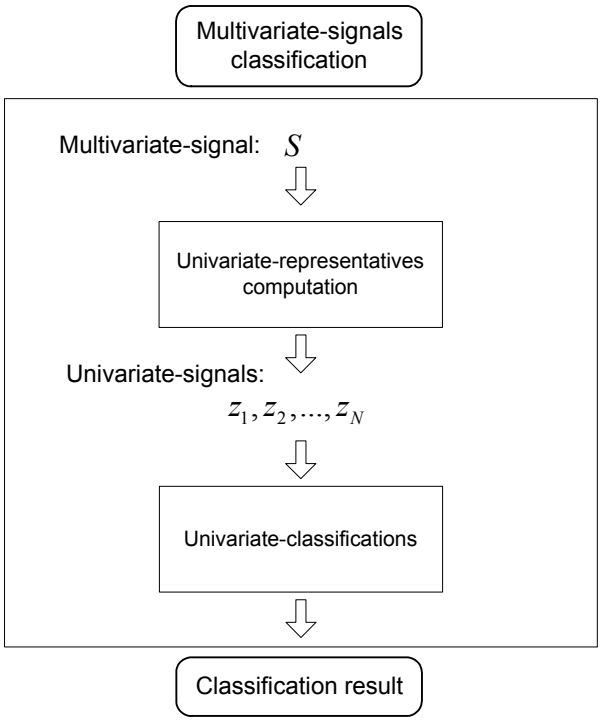

Figure 5. The multivariate-signals classification problem is transformed into several univariate-signal classifications.

In the following subsections we first present the univariate classification algorithm and then the decomposition of the multivariate signals into univariate representative signals.

5.1 Univariate signal classification in the time-frequency domain

In this subsection, the objects to be classified are univariate-signals (henceforth called simply signals).

Time-frequency representation

Time-frequency representations of a signal can be divided into two groups according to the nature of their transformations: linear (Short-time Fourier Transform), and quadratic (based on the Wigner-Ville distribution). Here we focus on the quadratic representation.
According to [16] all time-frequency representations (TFR) of a signal $s(t)$ can be obtained from[2]:

$$C(t,\omega) = \frac{1}{4\pi^2} \iiint s^*\left(u - \frac{1}{2}\tau\right) s\left(u + \frac{1}{2}\tau\right) \phi(\theta,\tau)\, e^{-j\theta t - j\tau\omega + j\theta u}\, du\, d\tau\, d\theta \qquad (2)$$

where: t is the time, ω is the frequency, τ is the time-lag (usually called doppler), θ is the frequency-lag (usually called delay) and $\phi(\theta,\tau)$ is a two dimensional function called the kernel.

The choice of the kernel is guided by the desire to have a time-frequency representation satisfying some established properties with regard to the application. Here, we designed a kernel with the objective of efficient signal classification.

There are a number of alternative ways for writing the general class of time-frequency distributions that are the most convenient for the classification application. One of them is the characteristic function formulation. We recall that the characteristic function $M(\theta,\tau)$ is the double Fourier transform of the TFR [16].

[2] All the integrals where the limits are not indicated span from $-\infty$ to $+\infty$.

$$C(t,\omega)=\frac{1}{4\pi^2}\iint M(\theta,\tau)e^{-j\theta t-j\tau\omega}d\theta d\tau \tag{3}$$

combining Eqs. 2 and 3 we obtain:

$$M(\theta,\tau)=\phi(\theta,\tau)\iint s^*\left(u-\frac{1}{2}\tau\right)s\left(u+\frac{1}{2}\tau\right)e^{j\theta u}du=\phi(\theta,\tau)\,A(\theta,\tau) \tag{4}$$

where $A(\theta,\tau)$ is the symmetrical ambiguity function of $s(t)$ defined as:

$$A(\theta,\tau)=\int s^*\left(u-\frac{1}{2}\tau\right)s\left(u+\frac{1}{2}\tau\right)e^{j\theta u}du=\int \hat{s}^*\left(\omega+\frac{1}{2}\theta\right)\hat{s}\left(\omega-\frac{1}{2}\theta\right)e^{j\tau\omega}d\omega \tag{5}$$

and $\hat{s}(\omega)$ is the Fourier transform of $s(t)$.

Equation 5 allows us to interpret the ambiguity function (AF) as a measure of the joint time-frequency auto-correlation of $s(t)$. The $\theta-\tau$ plane is commonly called ambiguity-plane.

The kernel function that can be seen as a mask in the ambiguity-plane has the goal of enhancing the regions in the plane $\theta-\tau$ that better discriminate the signals to be classified.
In this research we consider the classification problem with respect to the modulus of the characteristic-function (CF). The kernel is then designed so as to enhance the regions where this modulus is more discriminative.

Kernel design

Given a training set $\Upsilon=\left\{s_{w_1}^{q_1}(t),s_{w_2}^{q_2}(t),...,s_{w_W}^{q_W}(t)\ ;\ q_k=1,...,Q_{w_k};1\le k\le W\right\}$ of labeled signals; where W is the number of classes, Q_{w_k} the number of labeled signals belonging to class w_k, and $s_{w_k}^{q_k}(t)$ the q_k^{th} signal belonging to class w_k. We wish to determine a kernel function $\phi(\theta,\tau)$ so that we can compare the CF-modulus of an unknown signal $s(t)$ to that of each class and assign $s(t)$ to its most likely class.

We define the set $AFM(\Upsilon)$ as:

$$AFM(\Upsilon)=\left\{\left|A_{w_1}^{q_1}(\theta,\tau)\right|,\left|A_{w_2}^{q_2}(\theta,\tau)\right|,...,\left|A_{w_W}^{q_W}(\theta,\tau)\right|\ \ ;\ \ q_k=1,...,Q_{w_k}\ ;1\le k\le W\right\}$$

where $A_{w_k}^{q_k}(\theta,\tau)=\int\left(s_{w_k}^{q_k}\left(t-\frac{\tau}{2}\right)\right)^*s_{w_k}^{q_k}\left(t+\frac{\tau}{2}\right)e^{j\theta t}dt$

In order to detect the regions where the class differences are maximal, we define the contrast function $\Gamma(\theta,\tau)$ as:

$$\Gamma(\theta,\tau)=\frac{\sum_{1\le k1<k2\le W}\left|E\left[\left|A_{w_{k1}}(\theta,\tau)\right|\right]-E\left[\left|A_{w_{k2}}(\theta,\tau)\right|\right]\right|^2}{\sum_{k=1}^{W}VAR\left[\left|A_{w_k}(\theta,\tau)\right|\right]} \qquad \text{.....(6)}$$

where

$E\left[\left|A_{w_k}(\theta,\tau)\right|\right]=\frac{1}{Q_{w_k}}\sum_{q_k=1}^{Q_{w_k}}\left|A_{w_k}^{q_k}(\theta,\tau)\right|$ is the mean AF-modulus corresponding to class w_k.

$VAR\left[\left|A_{w_k}(\theta,\tau)\right|\right]=\frac{1}{Q_{w_k}}\sum_{q_k=1}^{Q_{w_k}}\left(\left|A_{w_k}^{q_k}(\theta,\tau)\right|-E\left[\left|A_{w_k}(\theta,\tau)\right|\right]\right)^2$ is the variance of the AF-modulus corresponding to class w_k.

The discrete version of the $\theta-\tau$ plane allows us to select the κ points of maximum contrast.
We group these points in a max-contrast set *K* defined as:

$$K=\left\{(m_1\cdot\Delta\theta,n_1\cdot\Delta\tau),(m_2\cdot\Delta\theta,n_2\cdot\Delta\tau),...,(m_\kappa\cdot\Delta\theta,n_\kappa\cdot\Delta\tau)\right\}\ \text{such as}$$

$$\Gamma(m_1\cdot\Delta\theta,n_1\cdot\Delta\tau)\ge\Gamma(m_2\cdot\Delta\theta,n_2\cdot\Delta\tau)\ge...\ge\Gamma(m_\kappa\cdot\Delta\theta,n_\kappa\cdot\Delta\tau)$$

where $\Delta\theta$ and $\Delta\tau$ are the discretization steps.

We design the kernel as a discrete binary function where the points in K are set to "1" while the others are set to "0".

$$\phi(m\cdot\Delta\theta, n\cdot\Delta\tau)=\begin{cases}1 \;\; if \;\; (m\cdot\Delta\theta, n\cdot\Delta\tau)\in K\\ 0 \;\; otherwise\end{cases}$$

Class model

The model of the class w_k is composed of its mean AF-modulus, its variance AF-modulus and the kernel. All these elements are considered in their discrete form.

By an adequate choice of units, we can set the discretization steps $\Delta\theta$ and $\Delta\tau$ to 1.

The model of the class w_k can be written as follows:

$$Model(w_k)=\left\{E\left[\left|A_{w_k}(m,n)\right|\right], VAR\left[\left|A_{w_k}(m,n)\right|\right], \phi(m,n)\right\}$$

In an alternative way, the set K can be included instead of $\phi(m,n)$.

$$Model(w_k)=\left\{E\left[\left|A_{w_k}(m,n)\right|\right], VAR\left[\left|A_{w_k}(m,n)\right|\right], K\right\}$$

Unlabeled signals classification

In order to assign an unknown signal $s(t)$ to a class we need a distance measure between $s(t)$ and a class-model. We take as a distance measure:

$$d\left(s(t), \text{model}(w_k)\right)=\sum_{(m_i,n_i)\in K}\frac{\left(\left|A(m_i,n_i)\right|-E\left[\left|A_{w_k}(m_i,n_i)\right|\right]\right)^2}{VAR\left[\left|A_{w_k}(m_i,n_i)\right|\right]}=d^s_{w_k} \tag{7}$$

where $\left|A(m_i,n_i)\right|$ is the discrete AF-modulus of $s(t)$ at point (m_i,n_i).

In fact $d^s_{w_k}$ is the Mahalanobis distance between the AF-modulus of $s(t)$ and the mean AF-modulus of class w_k at the points where the kernel $\phi(m,n)$ is different from zero.

The most likely class of $s(t)$ is given by its classification defined by:

$$classification(s(t))=\underset{w_k}{\text{argmin}}\left(d^s_{w_k}\right) \tag{8}$$

Classification error rate

The classification error rate is defined, with respect to a labeled signal set (test set), by the ratio between the number of correctly classified signals and the total number of signals in the labeled set.

The choice of the parameter κ (number of contrast points that we take into account) remains to be detailed. This parameter should be chosen so as to minimize the classification error in a test set of labeled signals. This can be achieved by increasing the value of κ until a minimal classification error rate is obtained.

5.2 Multivariate signal classification in the time frequency domain

A multivariate-signal (MVS) $S(t)$ can be written in a vector-form; $S(t)=\left[s_1(t),...,s_N(t)\right]^t$, where the $s_i(t)$ are the components of $S(t)$. We can easily adapt the formulation in Subsect. 3.1, of the univariate-classification problem to the multivariate case as follows.

Given a training set of labeled MVSs; $\Upsilon=\left\{S^{q_1}_{w_1}(t), S^{q_2}_{w_2}(t),...,S^{q_W}_{w_W}(t)\;;\; q_k=1,...,Q_{w_k}\;;\; 1\le k\le W\right\}$; where W is the number of classes, Q_{w_k} the number of labeled MVSs belonging to class w_k, and $S^{q_k}_{w_k}(t)$ the q_k^{th} MVS belonging to class w_k. We wish to characterize each class by a model so that we can compare an unknown MVS $S(t)$ to each class-model and assign $S(t)$ to its most likely class.

Time-frequency- space representation of multivariate signals

The multivariate ambiguity function (MAF) of a MVS $S(t)$ is defined by [17]:

$$MA(\theta,\tau)=\int S\left(t+\frac{\tau}{2}\right)S^{H}\left(t-\frac{\tau}{2}\right)e^{j\theta t}dt \tag{9}$$

where ^{H} stands for conjugate transpose.

Another way to write Eq.9 in a matrix form is presented below

$$MA(\theta,\tau)=\begin{bmatrix} \int s_1{}^{*}\left(t-\frac{\tau}{2}\right)s_1\left(t+\frac{\tau}{2}\right)e^{j\theta t}dt & \dots & \int s_N{}^{*}\left(t-\frac{\tau}{2}\right)s_1\left(t+\frac{\tau}{2}\right)e^{j\theta t}dt \\ \dots & \dots & \dots \\ \int s_1{}^{*}\left(t-\frac{\tau}{2}\right)s_N\left(t+\frac{\tau}{2}\right)e^{j\theta t}dt & \dots & \int s_N{}^{*}\left(t-\frac{\tau}{2}\right)s_N\left(t+\frac{\tau}{2}\right)e^{j\theta t}dt \end{bmatrix} \tag{10}$$

In Eq. 10 the terms on the diagonal are the auto-ambiguity functions (commonly called ambiguity functions) and the off-diagonal terms are called cross-ambiguity functions.

In Subsect. 4.1 we mentioned the fact that the ambiguity function could be interpreted as a measure of the joint time-frequency auto-correlation. The generalization of this interpretation implies that the MAF is an indicator of the joint time-frequency-space autocorrelation of a multivariate signal. The space dimension is taken into account by the cross-ambiguity functions.

Spatial decorrelation

A common approach when dealing with multivariate data is to find a number of components, satisfying some statistical properties that can generate the original multivariate data by applying a linear transformation. The most common techniques are the Principal Component Analysis (PCA) whose components are linearly statistically independent and Independent Component Analysis (ICA) whose components are statistically independents.

In both PCA and ICA the correlation between the new transformed components is zero. Therefore PCA and ICA lead to MVS whose components are spatially *decorrelated*.

Furthermore the MAF matrix of a spatial decorrelated MVS is diagonal.

Beside PCA and ICA, other decorrelation methods can be used. As in the case of the kernel design we can design a decorrelation method whose goal is to find components that maximally discriminate among the classes. A way to achieve this goal is to use a feature extraction based on eigenvector analysis [18]. An example of application in the BCI framework can be found in [19], where an interpretation in terms of spatial filters is presented. However, only two classes can be classified at a time.

We present below a decorrelation method based on the joint diagonalization of the autocorrelation matrices of each class.

We note by $Z(t)$ the transformed MVS (TMVS) resulting of the pre-multiplication of $S(t)$ by the matrix P .

$$Z(t)=P\cdot S(t) \tag{11}$$

The labeled MVS belonging to the training set Υ are P-projected to generate the transformed set $P\Upsilon$.

$P\Upsilon=\left\{Z_{w_1}^{q_1}(t),Z_{w_2}^{q_2}(t),\dots,Z_{w_W}^{q_W}(t)\ ;\ q_k=1,\dots,Q_{w_k};1\le k\le W\right\}$ where $Z_{w_k}^{q_k}(t)=P\cdot S_{w_k}^{q_k}(t)$

The signal components (transformed components) of $Z_{w_k}^{q_k}(t)$ are: $\left\{{}^{\ell}z_{w_k}^{q_k}(t)\ ;\ 1\le\ell\le N\right\}$

The discrete version of the set $P\Upsilon$ is constituted of the matrices $Z_{w_k}^{q_k}$ whose elements are the values of $Z_{w_k}^{q_k}(t)$ at the sampling instants.

We wish to determine the matrix P such that:

$$E\left[Z_{w_k}\cdot Z_{w_k}^t\right]=P\cdot E\left[S_{w_k}\cdot S_{w_k}^t\right]\cdot P^t=P\cdot\left(\frac{1}{Q_{w_k}}\sum_{q_k=1}^{Q_{w_k}}S_{w_k}^{q_k}\cdot\left(S_{w_k}^{q_k}\right)^t\right)\cdot P^t=P\cdot R_{w_k}\cdot P^t=D_{w_k}\ ;\ k=1...W \qquad (12)$$

where D_{w_k} are diagonal matrices and R_{w_k} is called the autocorrelation matrix of the class w_k. Thus the matrix P simultaneously diagonalizes the set $\left\{R_{w_k}\middle|1\le k\le W\right\}$.

As a matter of fact the matrix P that exactly diagonalizes this set exists when the R_{w_k} are normal[3] commuting matrices [20]. According to Eq. 12 the R_{w_k} are normal but they do not necessarily commute. However, it is possible to find a matrix that approximately diagonalizes the set $\left\{R_{w_k}\middle|1\le k\le W\right\}$ [20] by optimizing a joint diagonality criterion (minimization of the square sum of the off-diagonal elements). An iterative procedure consisting in the application of plane rotations so as to satisfy the joint-diagonality criterion is presented in [20]. Because of its efficiency and good results of such method we used it in our work.

In order to characterize the discrimination potential of each of the components of $Z(t)$; we define the contrast function $\Omega(\ell)$ where $\ell=1,...,N$ is the transformed-component index.

$$\Omega(\ell)=\frac{\sum_{1\le k1<k2\le W}\left(E\left[\int\left({}^{\ell}z_{w_{k1}}(t)\right)^2dt\right]-E\left[\int\left({}^{\ell}z_{w_{k2}}(t)\right)^2dt\right]\right)^2}{\sum_{k=1}^{W}VAR\left[\int\left({}^{\ell}z_{w_k}(t)\right)^2dt\right]}\ ;\ 1\le\ell\le N \qquad (13)$$

The function $\Omega(\ell)$ measures the contrast of the ℓ^{th} transformed-component when the energy in that component is used as discrimination parameter between the classes.

The contrast measure allows us to assign a classification-weight ρ_ℓ to each transformed component (Eq. 14).

$$\rho_\ell=\frac{\Omega(\ell)}{\sum_{l=1}^{N}\Omega(l)} \qquad (14)$$

Class model

The model of the class w_k is composed of the projection matrix P, the set of classification weights $\left\{\rho_\ell\middle|1\le\ell\le N\right\}$ and the univariate model of each component (see Subsect. 4.1).

$$Model\left(w_k\right)=\left\{P,\rho(\ell),E\left[\left|{}^{\ell}A_{w_k}(m,n)\right|\right],VAR\left[\left|{}^{\ell}A_{w_k}(m,n)\right|\right],{}^{\ell}K\ ;\ 1\le\ell\le N\right\}$$

where $E\left[\left|{}^{\ell}A_{w_k}(m,n)\right|\right]$, $VAR\left[\left|{}^{\ell}A_{w_k}(m,n)\right|\right]$ and ${}^{\ell}K$ are respectively: the mean AF-modulus of the ℓ^{th} component associated to the class w_k, the variance AF-modulus of the ℓ^{th} component associated to the class w_k and the max-contrast set of the ℓ^{th} component.

Unlabeled signals classification

Given a MVS $S(t)$ we first compute its TMVS $Z(t)$ (see Eq. 11) and obtain the transformed components $z_1(t),z_2(t),...,z_N(t)$.

Then the distances between each component and the model of each class associated with that component are calculated.

$$d_{w_k}^{\ell}=\sum_{(m_i,n_i)\in K_\ell}\frac{\left(\left|{}^{\ell}A(m_i,n_i)\right|-E\left[\left|{}^{\ell}A_{w_k}(m_i,n_i)\right|\right]\right)^2}{VAR\left[\left|{}^{\ell}A_{w_k}(m_i,n_i)\right|\right]} \qquad (15)$$

[3] A matrix A is normal when $A=A^H$

where $\left|{}^{\ell}A(m_i, n_i)\right|$ is the modulus of the AF of $z_\ell(t)$.

Finally the global distance between $S(t)$ and the class w_k is:

$$D_{w_k}^{S(t)} = \sum_{\ell=1}^{N} \rho(\ell) \cdot d_{w_k}^{\ell} \tag{16}$$

The most likely class of $S(t)$ is given by its classification defined as:

$$classification(S(t)) = \underset{w_k}{\operatorname{argmin}} \left(D_{w_k}^{S(t)} \right) \tag{17}$$

6 EXPERIMENTAL METHODS AND PROTOCOL

Two male and healthy volunteers (S1 and S2), 29 and 23 years old participated in six sessions of 20 minutes distributed over five weeks. The subjects were comfortably sitting in an armchair and placed in front of a computer screen. The experimentation room was quiet and slightly illuminated.

The subjects started each session by five minutes of the VOM. During the VOM we controlled the recording conditions and set the threshold parameters for artefact rejection (see Sect. 4). Furthermore, the VIS-OM allowed subjects to get familiar with the system.

The EEG signals were recorded with reference to digitally linked ears (see Subsect. 2.1) and from electrodes Fp1, Fp2, F3, F4 C3, C4, P3, P4, O1 and O2 of the 10/20 international system, at a rate of 256 Hz per channel. The electrodes Fp1 and Fp2 were used only for eye-movement artefacts detection and they were not included in the classification analysis.

Both subjects were asked to perform the following imagined mental activities: vertical movements of the left and right index fingers (MA1 and MA2) and incremental mental counting (MA3).

Visual cues were used to indicate which mental activity to perform. In the case of MA1 and MA2 an horizontal arrow pointing to the left or to the right was displayed on the computer screen; for MA3 the first two-digit number was displayed.

The first recording session was carried out without feedback and the next five with feedback. In the first session the first MA models were calculated; that allowed us to provide feedback in the second session. During the feedback sessions the MA models were updated incrementally as explained in Subsect. 6.2.

The temporal parameters T and T_1 were both set to 0.5-second (see Subsect. 2.3). The goal was therefore to train MA models able to correctly classify half-second EEG segments (trials).

6.1 Protocol of a training-without-feedback session

The first five minutes were spent with the VOM. The remaining 15 minutes were divided into three five-minute slices in which respectively MA1, MA2 and MA3 were trained.

The five-minute slices were as well divided into one-minute recordings and 30-second break as is depicted in Fig. 6. The one-minute recordings were organized in the following way: at the beginning the corresponding visual cue was displayed and lasted five seconds. Then a break-signal appeared, indicating five-second break. This process was repeated during the one-minute recording (Fig. 6).

At the end of this session the MA models for the three MAs were computed. These models are calculated as explained in Sect. 5.

Theoretically we have 180 trials per mental activity for training the MA models. However, the first trial after the presentation of the visual cue is rejected because of the presence of evoked potentials -due to visual stimulation- and about 20% of the trials are rejected because of artefacts. In practice no more than 150 trials per mental activity were available.

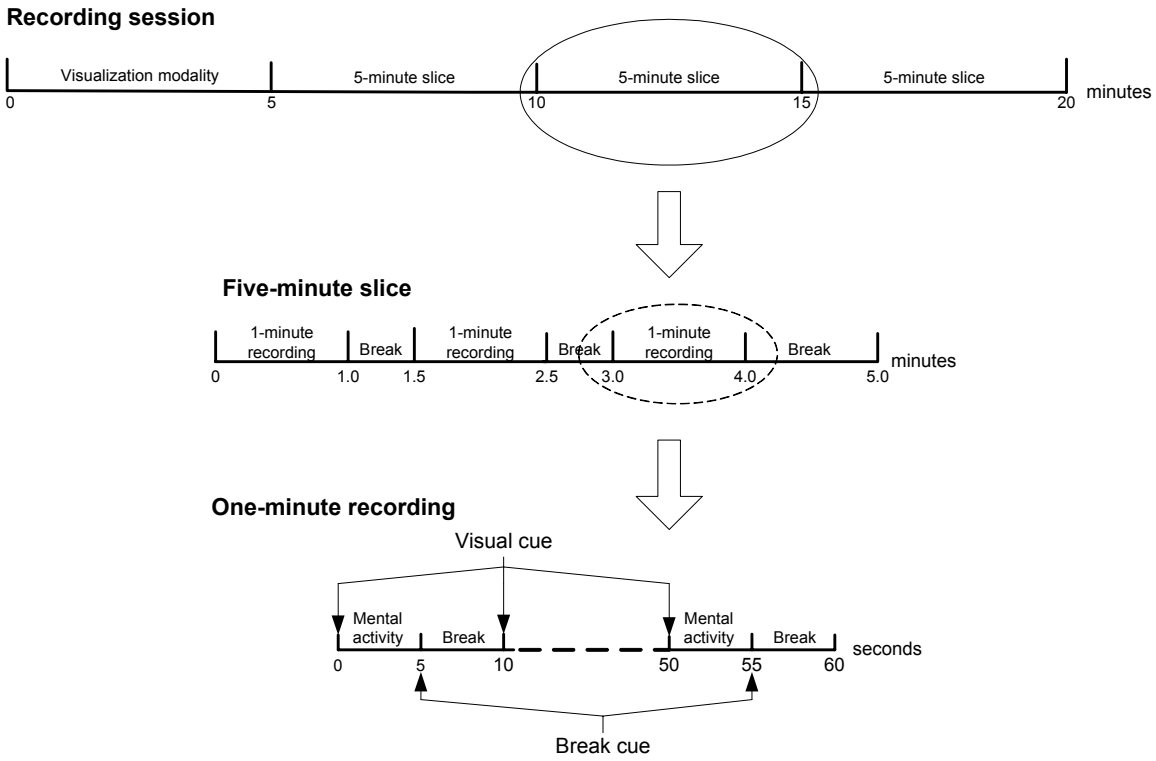

Figure 6. Protocol of a training without feedback.

6.2 Protocol of a training-with-feedback session

The 20 minutes are distributed between visualization, MAs and breaks in the same way as in the precedent case (Fig. 7).

During the MAs a feedback is provided to the subject in the form of a sphere that moves left, right or up-wards if MA1, MA2 or MA3, were correctly identified. If the MA was wrongly classified the sphere does not move. The feedback is provided for each half-second but the first after the visual cue indicating which MA to perform (see Fig. 7).

During the last break period of each five-minutes-slice the MA models are updated with the new recorded data.

Table 1 shows the MAs that were trained in each five-minute slices of the session with feedback.

Session / 5 min-slice	2	3	4	5	6
1	MA1	MA2	MA3	MA1	MA2
2	MA2	MA2	MA3	MA1	MA1
3	MA3	MA3	MA1	MA2	MA3

Table 1. Mental activities trained during the three five-minute slices of each feedback session.

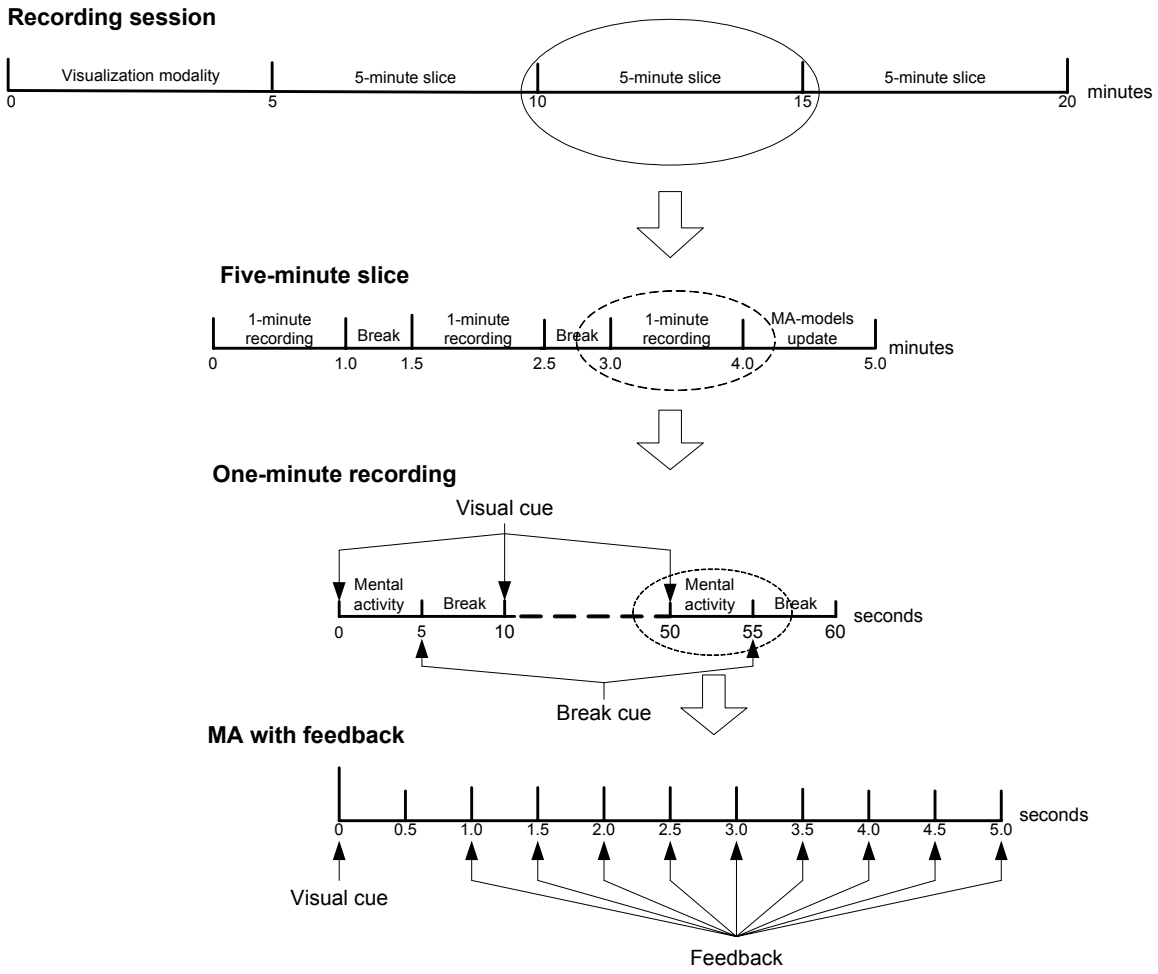

Figure 7. Protocol of a training with feedback.

7 RESULTS AND DISCUSSIONS

We divided the results presentation into two parts. The results of the first session where no feedback was provided and those of sessions where feedback was provided (two to six).

First session (without feedback)

The number of retained trials in the first session (after artefact rejection), per subject and per MA is reported in Table 2.

Mental activity / Subject	MA1	MA2	MA3
S1	149	144	148
S2	146	143	142

Table 2. Number of retained trials per subject and per MA in the first session (after artefact-rejection)

We used 100 trials to compute the matrix P , the mean AF-modulus and the variance AF-modulus of each transformed component (see Subsect. 5.2). The remaining trials were used as test set to determine the

optimal number of contrast points, in the ambiguity-plane, associated with each transformed component (TRC).

In Fig. 8 (for Subject 1) and Fig. 9 (for Subject 2) the absolute values of the coefficients of the matrix P are represented in a comparative graph (left). This graph gives us the information about the composition of each TRC as a linear combination of signals coming from different electrodes. In the right part, the classification weights associated with each TRC calculated according to Eq. 14 are depicted.

The results of Fig. 8 and Fig. 9 show that for both subjects there are five TRC that seems to be more important for the classification than the others (1, 2, 3, 5 and 8 for Subject 1 and 1,2,3,6 and 8 for Subject 2). In order to confirm this impression we computed the classification error associated with each TRC and the optimal number of contrast points. These results are shown in Fig. 10 (for Subject 1) and Fig. 11 (for Subject 2). From these results we can say that the smaller error rates correspond to those components with largest classification weights.

We also present the optimal contrast points for the four TRCs that have the smallest error-rate. Only the first quadrants were represented since the modulus of the AF is symmetric with respect to the origin.

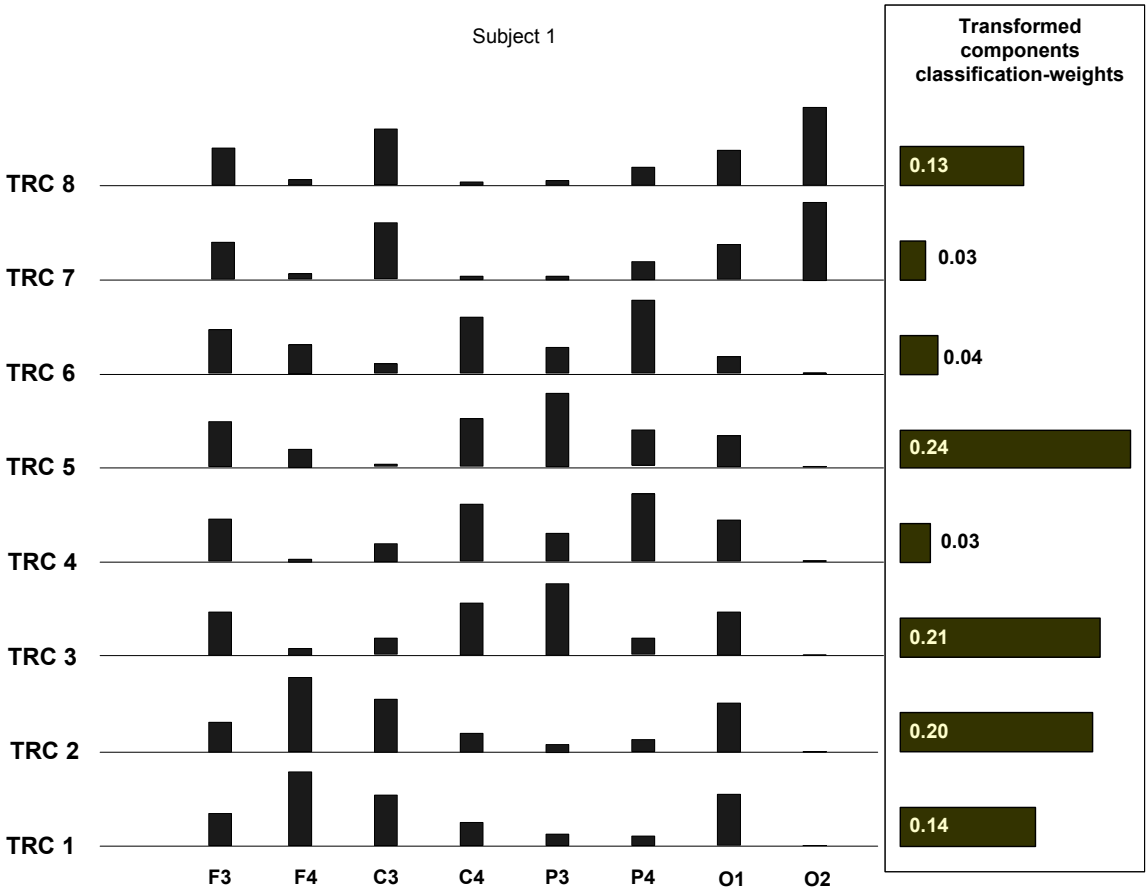

Figure 8. Results for Subject 1. Left: structure of the matrix P . Right: classification weights of each TRC.

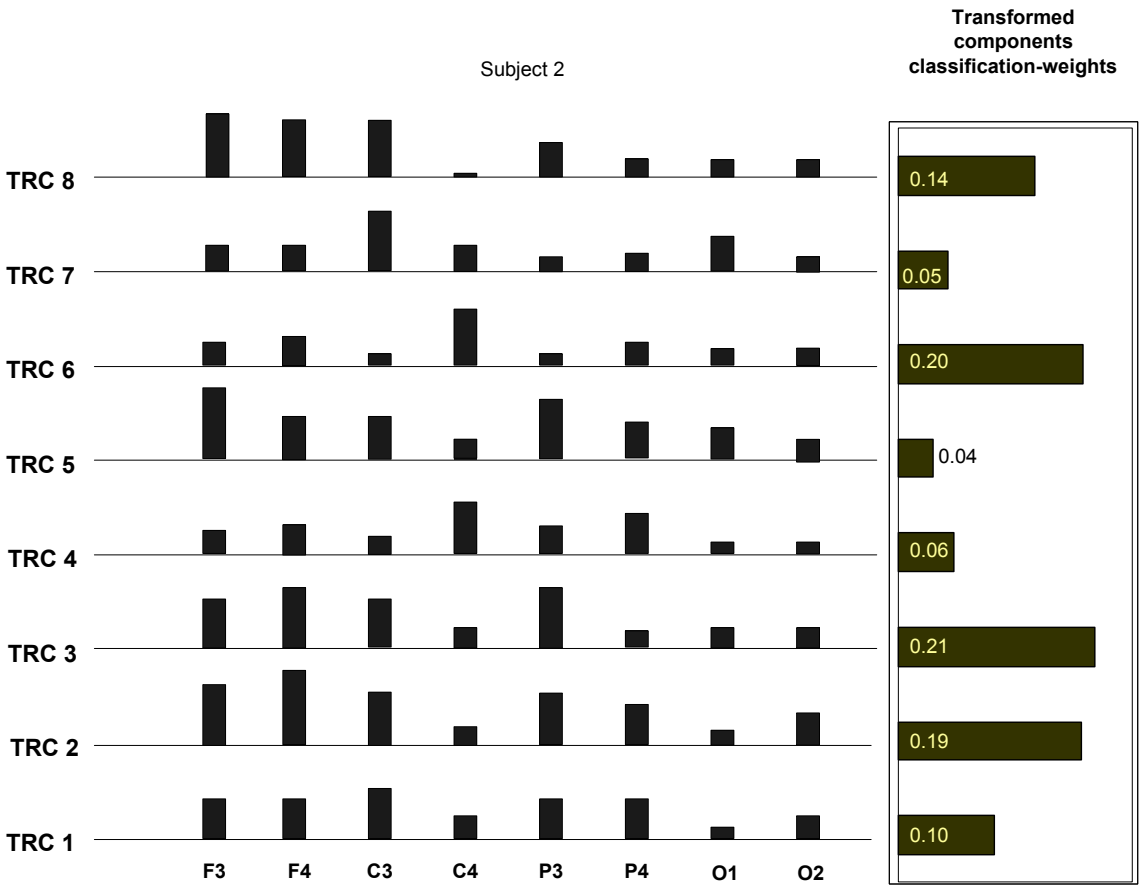

Figure 9. Results for Subject 2. Left: structure of the matrix P . Right: classification weights of each TRC.

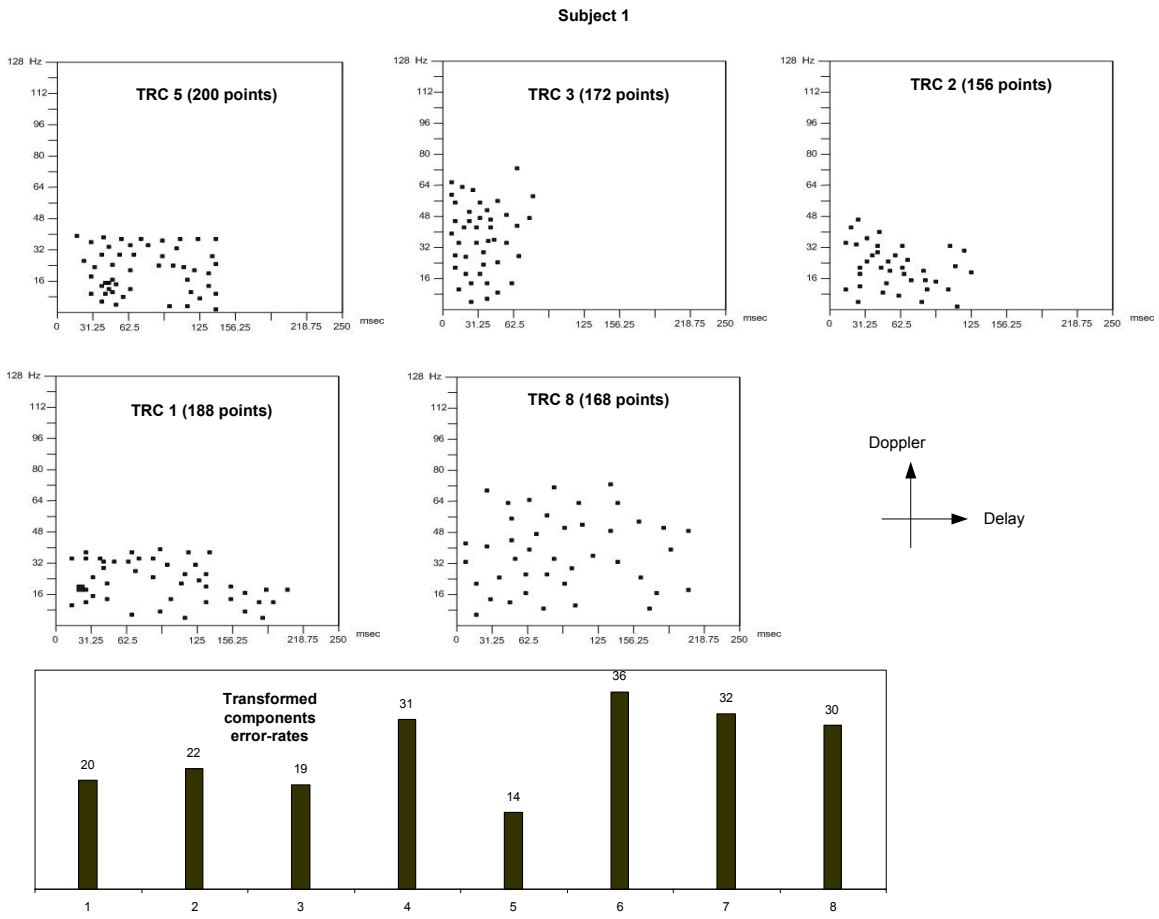

Figure 10. Top: Contrast points selected for the four TRC with the smallest error rates (as the modulus of the AF is symmetric with respect to the origin only the first quadrant is represented). Down: Error rates associated with each TRC (Subject 1).

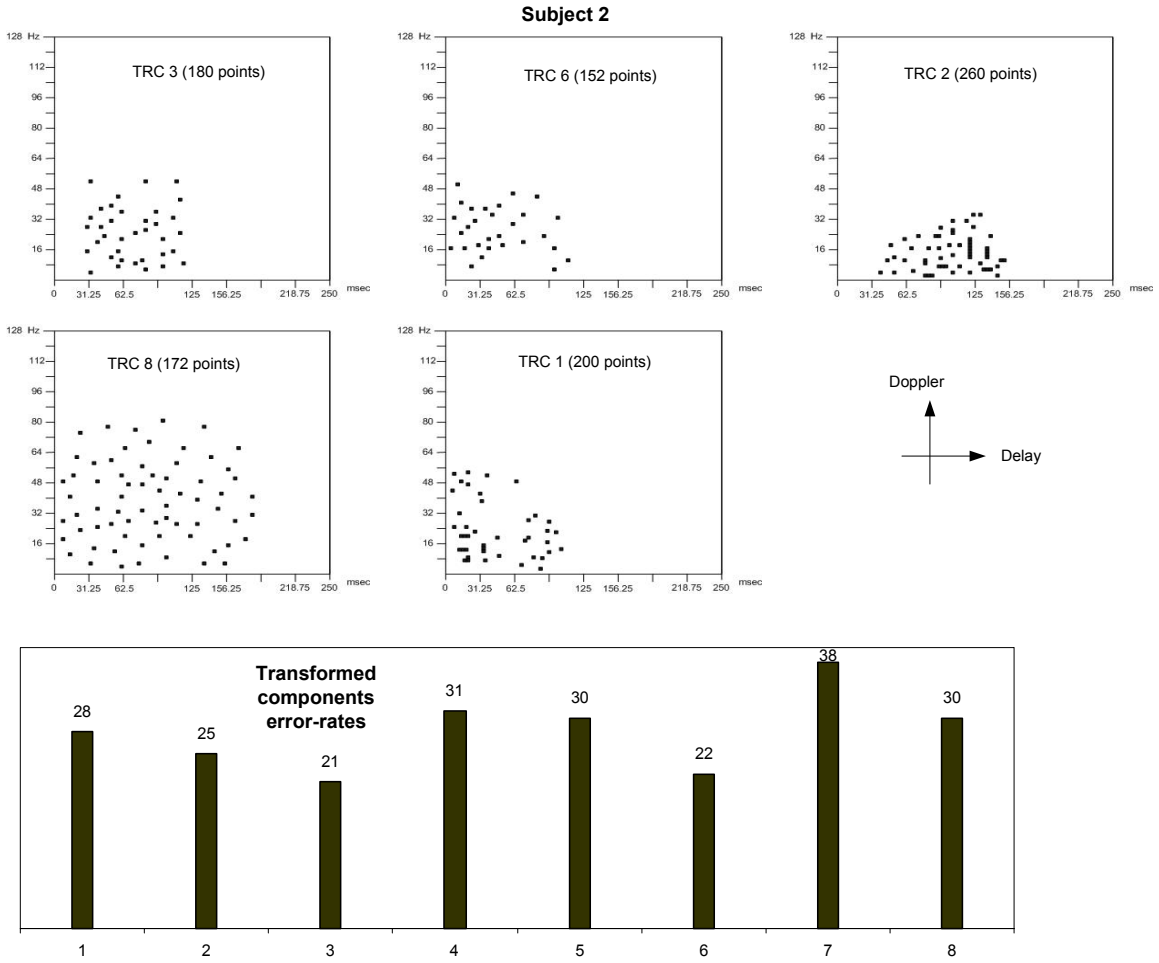

Figure 11. Top: Contrast points selected for the four TRC with the smallest error rates (as the modulus of the AF is symmetric with respect to the origin only the first quadrant is represented). Down: Error rates associated with each TRC (Subject 2).

Sessions from two to six (with feedback)

In table 3 we report the number of retained trials after artefact elimination for each five-minute slice from sessions two to six.

During the second session each MA was trained with feedback (see Table 1). Such feedback was produced by taking as reference the models built after the first session. In Table 4 we present the percentage of trials that were not correctly classified among the non-rejected trials (error-rate).

At the end of the second session, new MA models were built using 100 trials (randomly chosen) for to compute the matrix *P*, the mean AF-modulus and the variance AF-modulus. The test set composed of the remaining trials was used to compute the optimal-number of contrast-points.

In Figs. 11 (for Subject 1) and 12 (for Subject 2) we represent the coefficients of the matrix *P* and the contrast points for each of the five TRC that have the largest classification weights. We can see that the TRCs that have the largest classification weights are the same than in the case of the training without feedback (Figs. 7 and 8). This suggests that the relationship between the coefficients of the matrix *P* remained the same. In the case of contrast-points we can remark that the general distribution found during the training without feedback is generally maintained in the training with feedback. On the other hand, the optimal number of contrast points has slightly changed with respect to the training without feedback.

It is important to note that we built new MA models at the end of the second session in order to do it in feedback conditions. In this way it is possible to update the models after each five-minute slice in sessions from three to six.

From sessions three to six we updated the matrix *P*, the mean AF-modulus and the variance of the AF-modulus of the trained MA each five-minute slice. This procedure was performed by using 100 trials randomly chosen to update those parameters and to take the remaining trials as a test set for determining the optimal number of contrast points.

In Figs. 13 (Subject 1) and 14 (Subject 2) we represent the evolution of the error-rate over the sessions from three to six. The results are reported according to Table 1 i.e. each five-minutes-slice.

As it can be seen the error-rate decreased almost always except between sessions 3 and 4 for Subject 1. Nevertheless, at the end of the sixth session we achieved the lowest error-rates for all the MAs. This result suggests that the feedback strategy improved the performance of the system. In fact, the subjects reported their general satisfaction with regard to feedback because of its stimulating effects.

Subject 1

5 min-slice \ Session	2	3	4	5	6
1	145	141	142	147	148
2	147	151	144	148	144
3	150	152	150	149	146

Subject 2

5 min-slice \ Session	2	3	4	5	6
1	146	144	146	144	149
2	142	145	148	148	139
3	145	147	143	142	150

Table 3. Number of retained trials, after artefact-elimination, in the sessions where feedback was provided.

5 min-slice \ Subject	1	2
1	28	36
2	26	34
3	23	28

Table 4. Percentage of misclassified trials during the second session (first session where feedback was provided). The MA models used for producing feedback were those built after the first session where no feedback was provided

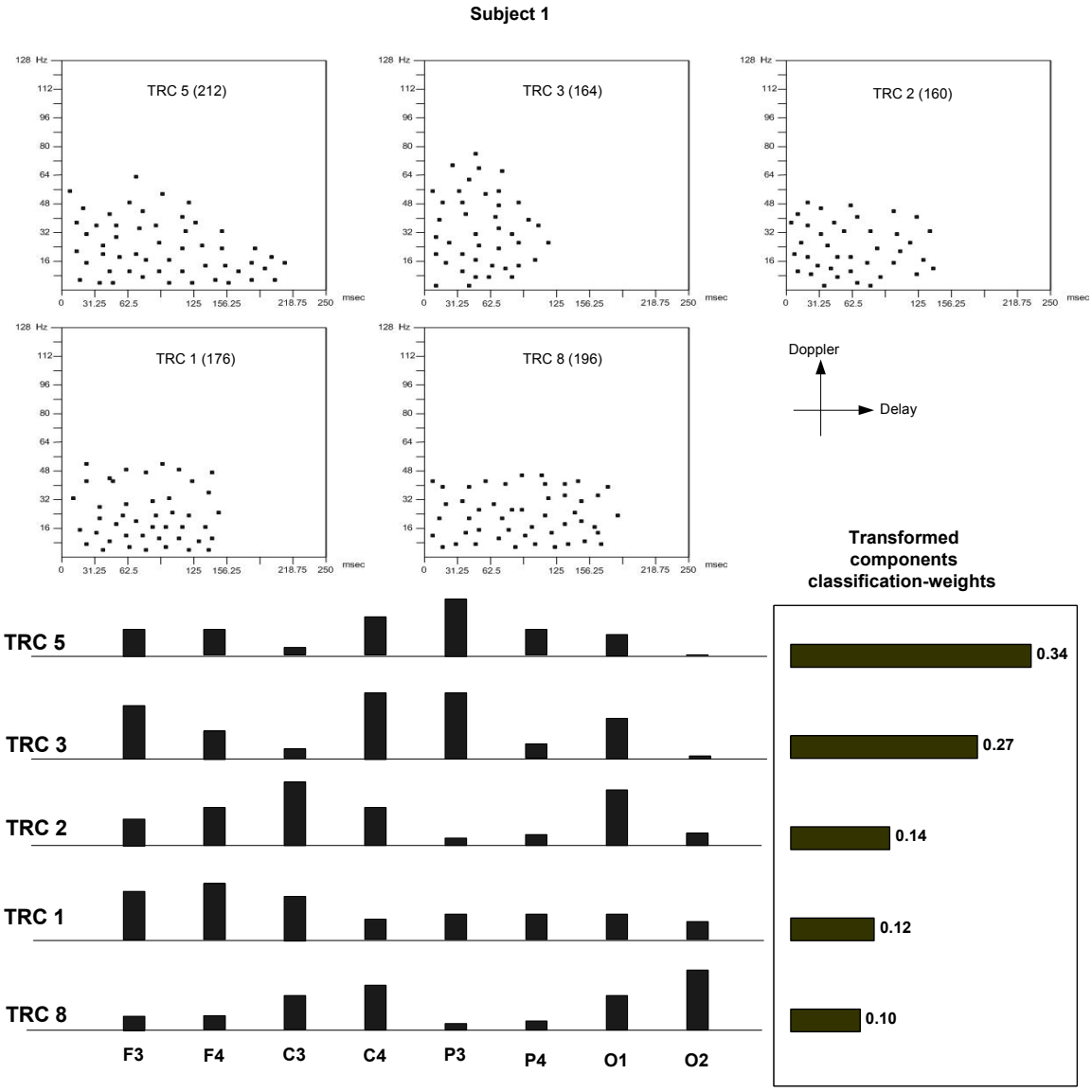

Figure 12. Results for Subject 1. TRCs with largest classification weights for the MA models built after the second session (first session with feedback). Top: Contrast points in the Doppler-delay plane. Middle: Rows of the matrix P associated with the TRCs. Down: Classification error-rate associated with each TRC.

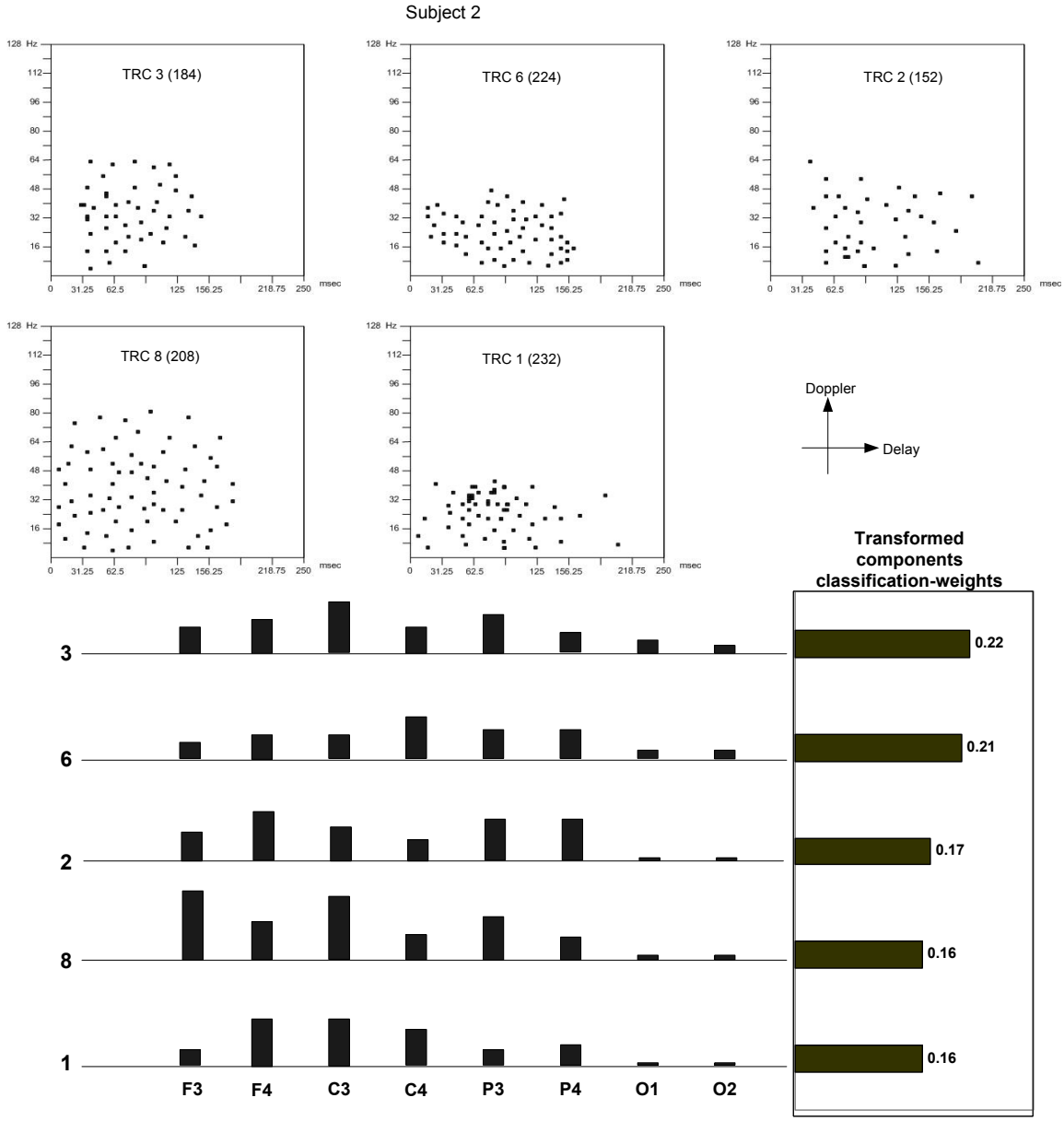

Figure 13. Results for Subject 2. TRCs with largest classification weights for the MA models built after the second session (first session with feedback). Top: Contrast points in the Doppler-delay plane. Middle: Rows of the matrix *P* associated with the TRCs. Down: Classification error-rate associated with each TRC.

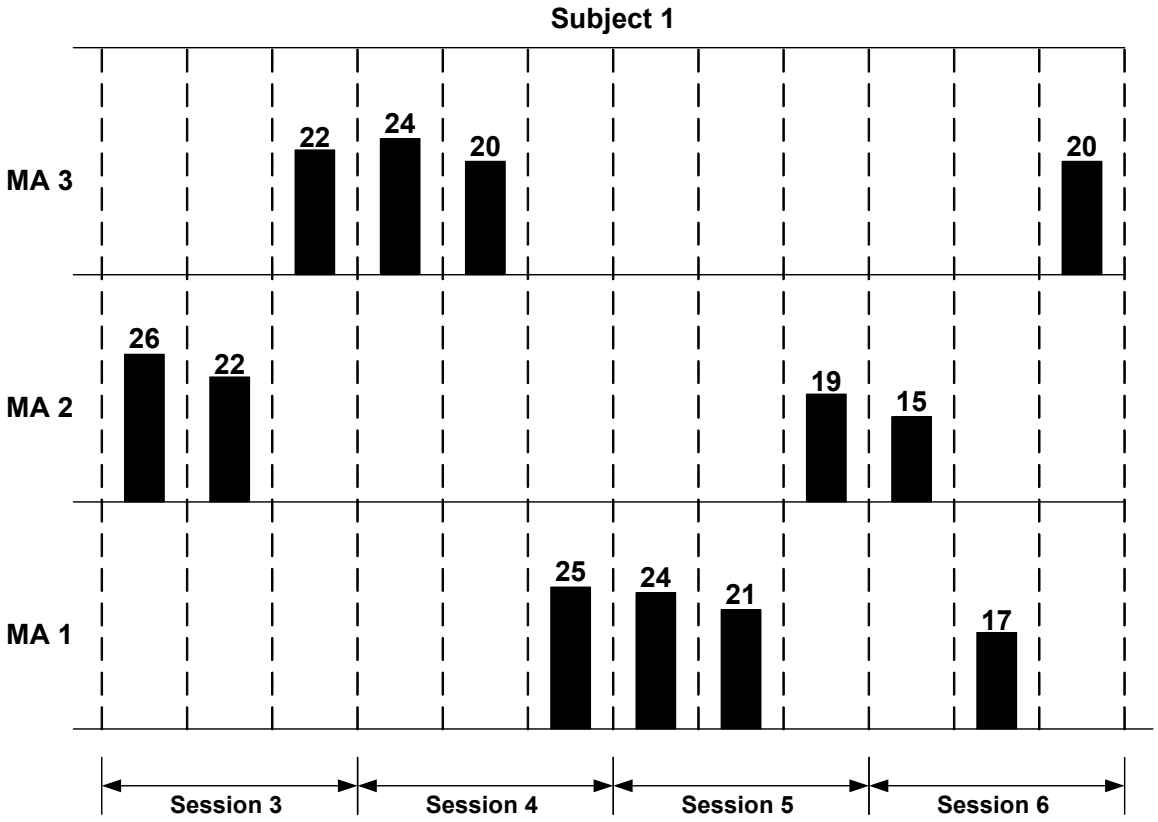

Figure 14. Error-rate evolution, for Subject 1, over the training sessions from three to six. We reported the error-rate for each five-minutes-slice according to Table 1.

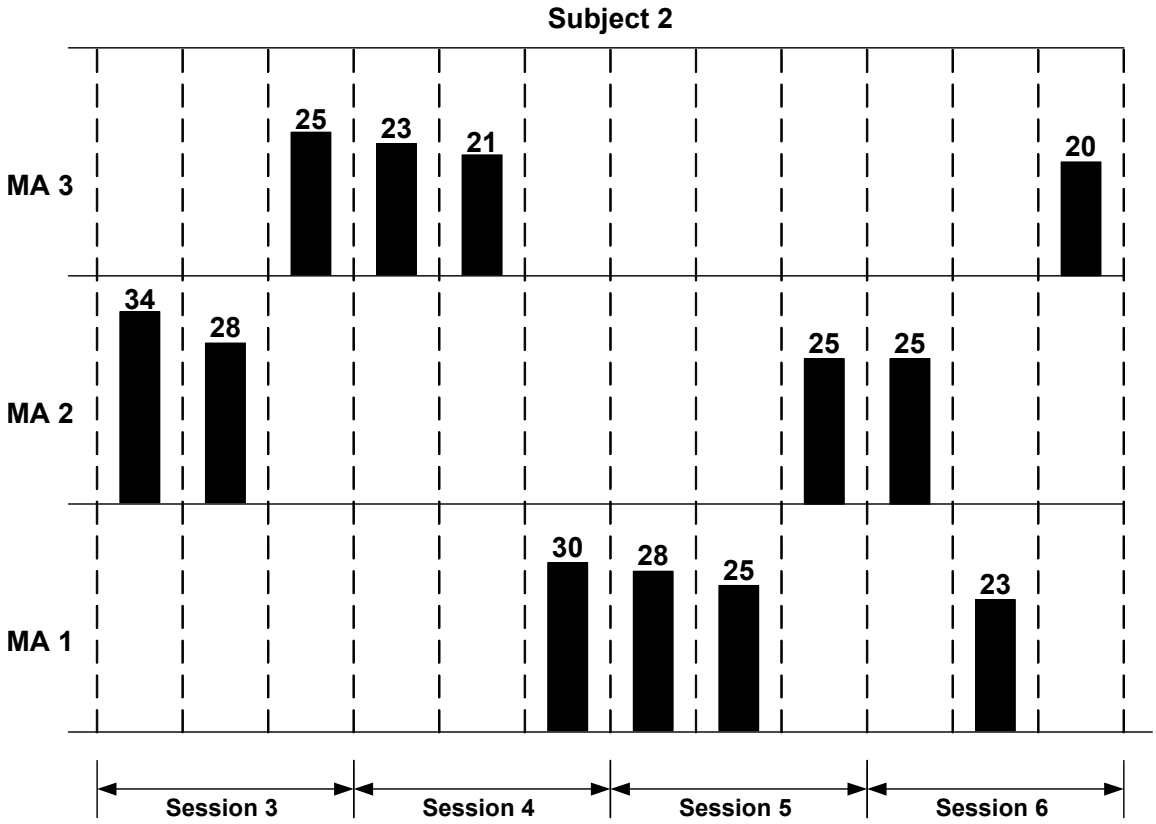

Figure 15. Error-rate evolution, for Subject 2, over the training sessions from three to six. We reported the error-rate for each five-minutes-slice according to Table 1.

8 CONCLUSIONS AND FUTURE WORK

In this paper we proposed a BCI system and an associated network architecture between the components that can be used in different operational modes. We stated that the relationship between these components should be flexible since the BCI technology is still in its experimental phase.

In order to familiarize the subjects with our BCI we proposed to precede each session with a short real-time visualization of a projection of the EEG signals in a 3D environment.

We classified EEG signals from the point of view of the joint correlation in three dimensions: time, frequency and space (as EEG signals are multivariate). In order to reduce the amount of data that results from such analysis we decorrelated the EEG signals before moving to the time-frequency correlation part. The decorrelation process resulted in a set of transformed components. In this way we divided the original problem of classification of multivariate signals into several univariate classifications.

The training was performed in two ways; with and without feedback. The results obtained show that the relationship between the transformed components remains essentially the same for both training types.

Nevertheless, as noticed in previous works [11] the structure of the MA models is different from person to person. Therefore, a BCI should be personalized.

The general reduction of the classification error rate over the sessions, where feedback was provided, shows that the feedback constituted an effective strategy for the training. Nevertheless, more experiments are necessary for confirming this hypothesis.

In the future we plan to experiment with more subjects during more sessions.

As the goal is to control devices by thinking, it is necessary to add more MAs for making possible, at least, a two-dimensional control.

We will consider other spatial analysis techniques such as non-linear PCA for extracting those transformed components that can be classified in the time-frequency domain.

Another possibility could be to perform a parametric time-frequency analysis (multivariate autoregressive models) first and then apply a spatial analysis technique.

9 ACKNOWLEDGEMENTS

The authors wish to acknowledge Patrick Aebischer and Guy Courbebaisse for fruitful discussions and suggestions which allowed us to improve the performance of our system. We would also like to thank the persons that participate in the experimental sessions.

10 REFERENCES

[1] J. D. Bayliss, "A Flexible Brain-Computer Interface", PhD Thesis University of Rochester, Rochester, New York, USA, 2001.
[2] M. Middendorf, et al, "Brain-Computer Interfaces Based on the Steady-State Visual-Evoked Response", *IEEE Trans. Rehab. Eng.*, Vol. 8, No. 2, pp. 211-214, June 2000
[3] A. Kübler, et al, "Self regulation of slow cortical potentials in completely paralyzed human patients", *Neuroscience Letters,* Vol. 252, pp. 171-174, 1998.
[4] G. Pfurtscheller, et al, "Current Trends in Graz Brain-Computer interface (BCI) Research", *IEEE Trans. Rehab. Eng.*, Vol. 8, No. 2, pp. 216-219, June 2000
[5] D. J. McFarland, et al, "An EEG-based method for graded cursor control", *Psychobiology,* 21:1, pp. 77-81, 1993.
[6] J. R. Wolpaw, et al, "Brain-Computer Interface Technology: A review of the first international meeting", *IEEE Trans. Rehab. Eng.*, Vol. 8, No. 2, pp. 164-173, June 2000.
[7] D.J. McFarland, et al, "Spatial filter selection for EEG-based communication", *Electroenceph. Clin. Neurophysiol.,* 103, pp. 386-394, 1997.
[8] J.F. Hair Jr., et al, Multivariate data analysis, Prentice Hall, New Jersey, 1998.
[9] J. R. Evans and A. Abarbanel, Introduction to Quantitative EEG and Neurofeedback, Academic Press, 1999.
[10] J. Robbins, "A Symphony in the Brain", Atlantic Monthly Press, New York, 2000.
[11] G. Garcia, T. Ebrahimi, J.-M. Vesin, "Classification of EEG Signals in the Ambiguity Domain for Brain-Computer Interface Applications", *to be published on IEEE Int. Conf. on Digit. Sig. Proc.,* Santorini, Greece, July 1-3 2002.
[12] M. Henning and S. Vinoski, Advanced CORBA® Programming with C++, Addison-Wesley professional computing series, 1999.
[13] T.P. Jung, et al, "Extended ICA removes artefacts from electroencephalographic recordings", *Advances in Neural Information Processing Systems*, Vol.10, pp. 894-900, 1998.
[14] M. van de Velde, et al, "Detection of muscle artefact in the normal human awake EEG", *Electroenceph. Clin. Neurophysiol.,* 107, pp. 149-158, 1998.
[15] L. Vigon, et al, "Quantitative evaluation of techniques for ocular artefact filtering of EEG waveforms", *IEEE Proc.-Sci. Meas. Technol.*, Vol. 147, No 5, September 2000.
[16] L. Cohen, Time-Frequency analysis, Prentice Hall Signal Processing Series, New Jersey, 1995.
[17] M.G. Amin, et al, "The Spatial ambiguity Function and Its Applications", *IEEE Sig. Proc Letters,* Vol. 7, No. 6, pp. 138-140, June 2000.
[18] C. W. Therrien, Decision estimation and classification, John Wiley & Sons, Inc., USA, 1989.
[19] H. Ramoser, et al, "Optimal Spatial Filtering of Single Trial EEG During Imagined Hand Movement", *IEEE Trans. Rehab. Eng.*, Vol. 8, No. 4, pp. 441-446, December 2000.
[20] J.-F. Cardoso, A. Souloumiac, "Jacobi Angles for Simultaneous Diagonalization", *SIAM J.Mat.Anal.Appl.*, vol. 17(1), pp. 161 ff, 1996.